Linear and Nonlinear Studies of EMHD instabilities driven by velocity shear

Amita Das

Institute for Plasma Research

Bhat, Gandhinagar – 382428

In collaboration with:

Neeraj Jain, Predhiman Kaw and Sudip Sengupta

Motivation

Shear driven EMHD instabilities occuring at fast time scales are relevant for Fast Ignition (FI) scheme of laser fusion. Nonlinear turbulent regime ~ may play a crucial role.

Fast Ignition

A variant of inertial confinement fusion scheme, where the task of compressing the nuclear DT pellet is separated from the creation of hot spot.

(a) Slow nsec laser pulse for compression.
(b) Fast sub-picosec laser pulse for ignition.

Comparison between conventional ICF and Fast Ignition.

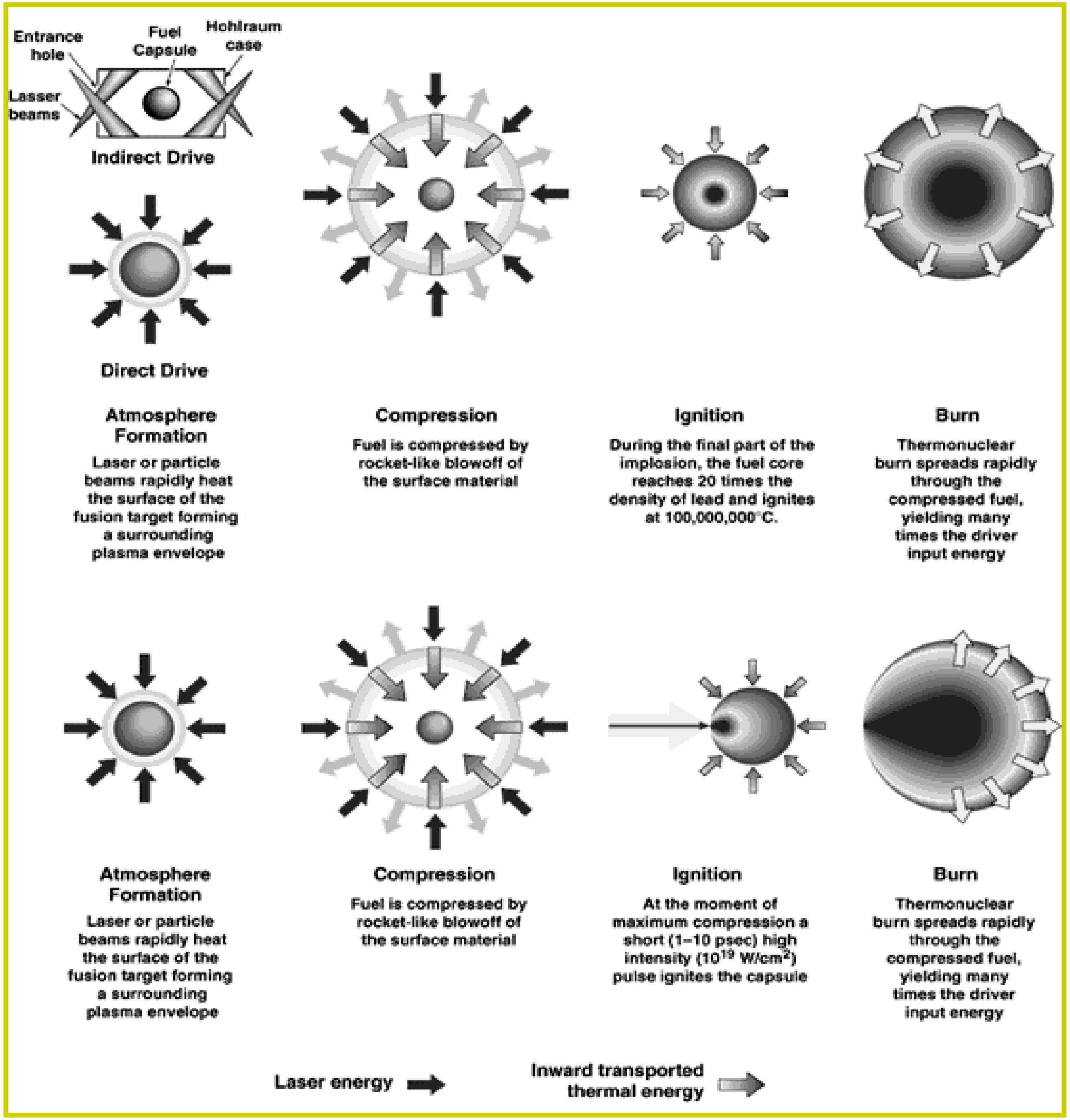

Advantages

- Compression easier – Core is not hot.
- Hydrodynamic instabilities (occurring during compression phase e.g. RT etc.) are inconsequential – fuel temperature same so no detrimental effect due to mixing.
- Relaxation of stringent requirements of spherical symmetry.

Key Question

(creation of the ignition spark)

- Pre – compressed target is over-dense for the ignitor laser pulse to penetrate.
- Creation of fast electrons at the critical density surface.
- FI scheme relies on the propagation of these fast electrons to the core for the creation of ignition spark.

Underlines the importance of the study of fast electron transport in plasmas!!

Beam transport

- Single particle collisions.
- Correlated collisions.
- Correction due to dense plasma.

Stopping distance estimate: Typically 100 – 1000 micron for 1 – 3 MeV beam

Typically larger than the target size.

Collective Plasma response

- Would be present.
- May even be necessary.

(As it can play a positive role by giving rise to anomalous stopping mechanisms through the generation of turbulence).

Evidences: collective response

- Scaled down experiments show a ten fold increase in neutron yield (Kodama et al. Nature).
- Experimental studies of Magnetic field evolution. (TIFR expts Sandhu et al. PRL 2002)
- PIC Simulations (Sentoku et al. PRE 200?)

Experimental Results
(Neutron yields)

Target	$E_{compress}$	No. beams	E_{heat}	Neutron output
Cone shell	1.2kJ	9	60J	$(1\text{-}3)\times10^5$
Cone Shell	1.2kJ	9	0	$(0.8\text{-}1)\times10^4$
Spherical shell only	2.6kJ	12	0	$(2\text{-}3)\times10^5$

Experimental evidence of anamolous stopping

TIFR Expt.

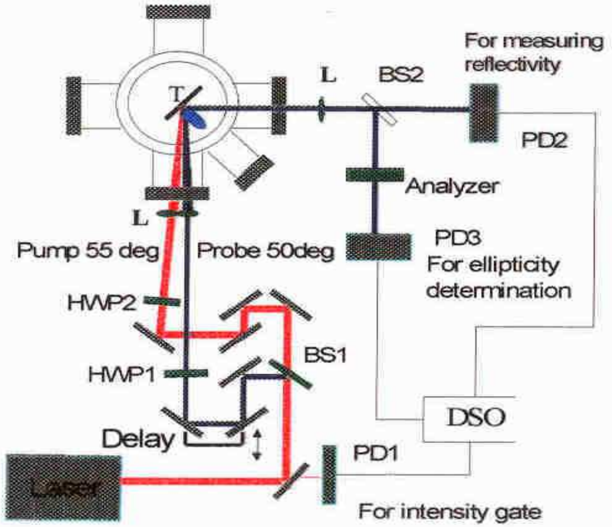

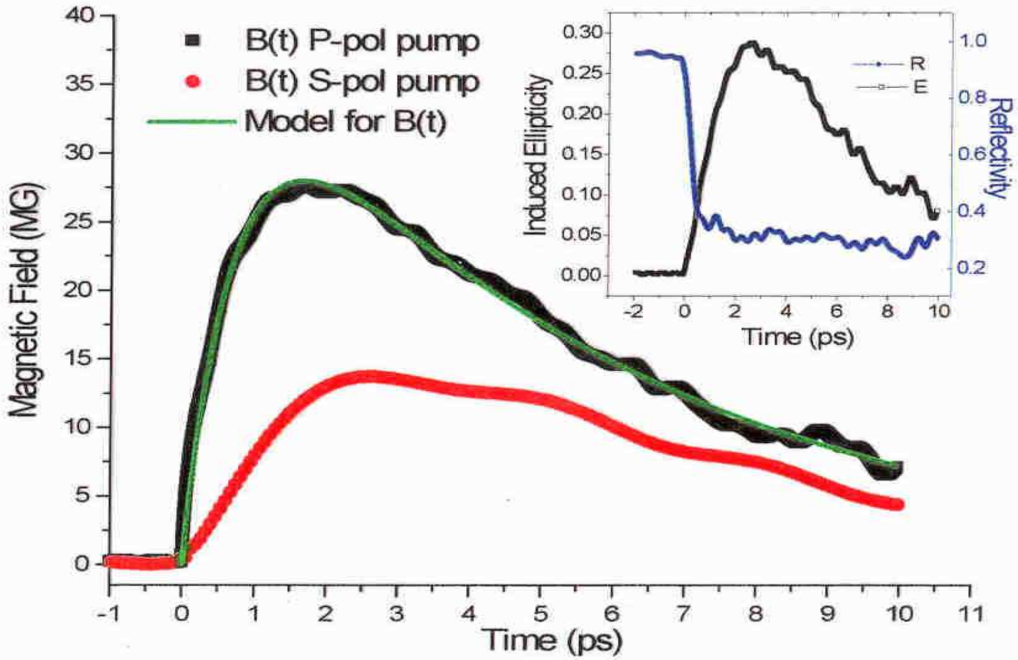

PRL 2002,
89 25thNov
issue

Sandhu et al (TIFR)
Sengupta et al (IPR)
Phys. Rev. Letters
(accepted 2002)

PIC Studies: Sentoku et al.

- As the energetic beam propagates inwards the background plasma electrons provides for the return shielding current in the opposite direction.
- The two currents get spatially separated as current sheets via Weibel instability.
- The current sheets tear and coalesce to form cylindrical current channels, core carrying inward current and outer shell the return current.
- PIC simulations show development of electromagnetic turbulence.
- Mechanism of turbulence generation unclear.

Current Channel

Schematic of flow configuration after Weibel, tearing and coalescence have occurred.

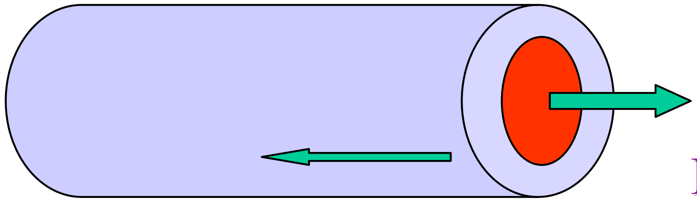

Equilibrium: Sheared axial Flow = $V_{0z}(r)$
Generates polloidal equilibrium magnetic field = $B_{\theta 0}(r)$
Look for shear driven instabilities at fast time scales!!

Governing Equations

- Fast time scale phenomena, ion response can be ignored. (Ions merely provide neutralizing background).
- Total current flow is due to electron motion.
- Governing equations Electron fluid momentum equation and Maxwell's equations.

Electron Magnetohydrodynamics(EMHD) Model: An Introduction

Governing Equations:

- Curl of Electron Momentum equation

$$\frac{\partial}{\partial t}\left(\nabla \times \vec{P}\right) = \nabla \times \left\{\vec{V}_e \times \left(\nabla \times \vec{P}\right)\right\} - m_e \nu \nabla \times \vec{V}_e$$

$$\vec{P} = \gamma_e m_e \vec{V}_e - e\vec{A}/c$$

here γ_e is the relativistic factor!

- Expression for current (immobile ions)

$$\vec{J} = -en_e V_e$$

- Ampere's Law

$$\nabla \times \vec{B} = 4\pi \vec{J}/c$$

Non relativistic limit

$$\Rightarrow \nabla \times \vec{P} = e\left(d_e^{\,2} \nabla^2 \vec{B} - \vec{B}\right)/c;$$

(where $d_e^2 = c^2/\omega_{pe}^{\;2}$)

Normalizations

- **<u>Length</u>:** Electron skin depth **($d_e = c/\omega_{pe}$)**
- **<u>Magnetic Field</u>:** Typical value **(B_{00})**
- **<u>Time</u>:**Corresponding gyroperiod **($eB_{00}/mc)^{-1}$**

Modes

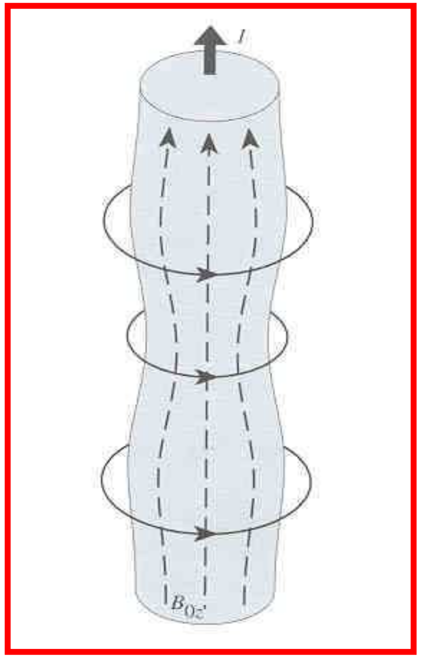

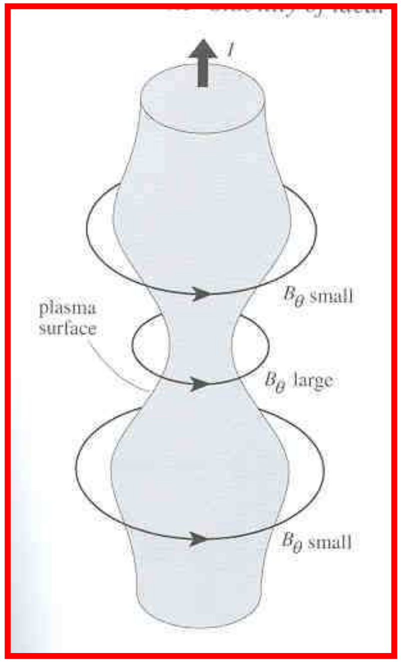

Sausage
2d perturbations

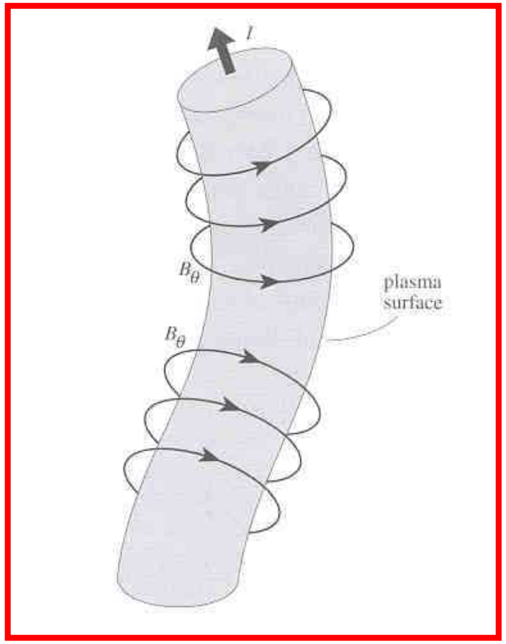

Kink
Generalized 3d perturbations

Region of analysis

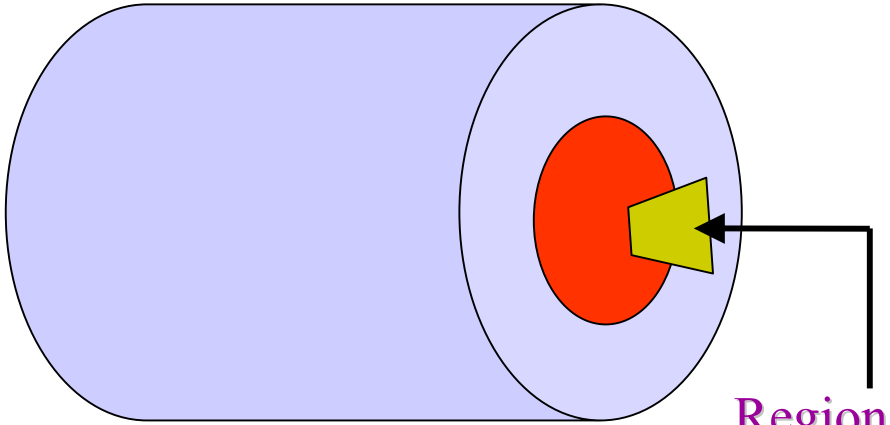

Equilibrium: Sheared axial Flow = $V_{0z}(x) = V_0 \tanh(x/\varepsilon)$
Generates equilibrium magnetic field along y = $B_{y0}(r)$

Axial : z
Radial : x
Poloidal : y

For 2d perturbation y taken as the symmetry direction.

EMHD Model in 2 dimensions

nonrelativistic

For two dimensional variations $\vec{B} = b\hat{\xi} + \hat{\xi} \times \nabla \psi$

EMHD equations reduce to following coupled set of equations for scalar fields b and ψ

$$\frac{\partial}{\partial t}\left(\psi - \nabla^2 \psi\right) + \hat{\xi} \times \nabla b \bullet \nabla\left(\psi - \nabla^2 \psi\right) = \eta \nabla^2 \psi$$

$$\frac{\partial}{\partial t}\left(b - \nabla^2 b\right) - \hat{\xi} \times \nabla b \bullet \nabla \nabla^2 b + \hat{\xi} \times \nabla \psi \bullet \nabla \nabla^2 \psi = \eta \nabla^2 b$$

$\psi_{eq} = 0$; $b_{eq} = B_{y0}$

Linearizing the EMHD equations for the sausage mode and Fourier analysing in time and 'Z' coordinate leads to:

$$\frac{d^2B}{dx^2}+3\frac{d\log(\gamma_0)}{dx}\frac{dB}{dx}-\frac{(1+\gamma_0 k_z^2)}{\gamma_0^3}B=\frac{k_z}{\gamma_0^3\varpi}\{V_0-(V_0\gamma_0)''\}B$$

Eq.(*)

B: Perturbed magnetic field along 'y'

V_0: Equilibrium flow along Z

γ_0: Relativistic factor $1/\sqrt{1-V_0^2}$

$\varpi = \omega - k_z V_0$

Additional terms in EMHD compared to Kelvin Helmholtz in hydrodynamics.

Second derivative of V_0 drives the instability

Necessary condition for instability

Multiplying Eq(*) by *B* and integrating by parts with respect to x gives

$$\int \left[\left(\frac{dB_{1y}}{dx} \right)^2 + (1+k_z^2) B_{1y}^2 \right] dx - \int \frac{k_z(v_0'' - v_0)}{\omega - k_z v_0} B_{1y}^2 \, dx = 0. \quad (8)$$

Equation (8) can then be satisfied for an imaginary value of ω only if the coefficient of ω_i vanishes (where ω_i represents the imaginary part of ω), all other terms being real in the equation. This implies

$$\int \frac{(v_0 - v_0'')}{|\omega - k_z v_0|^2} |B_{1y}|^2 \, dx = 0. \quad (10)$$

Hence, a necessary requirement for instability is that $v_0 - d^2v_0/dx^2$ should change sign, all other factors being positive in the integrand.

Summary of 2d linear Results

Local Analysis: Shear scale length >> Perturbation scale → No Instability

Non Local Analysis

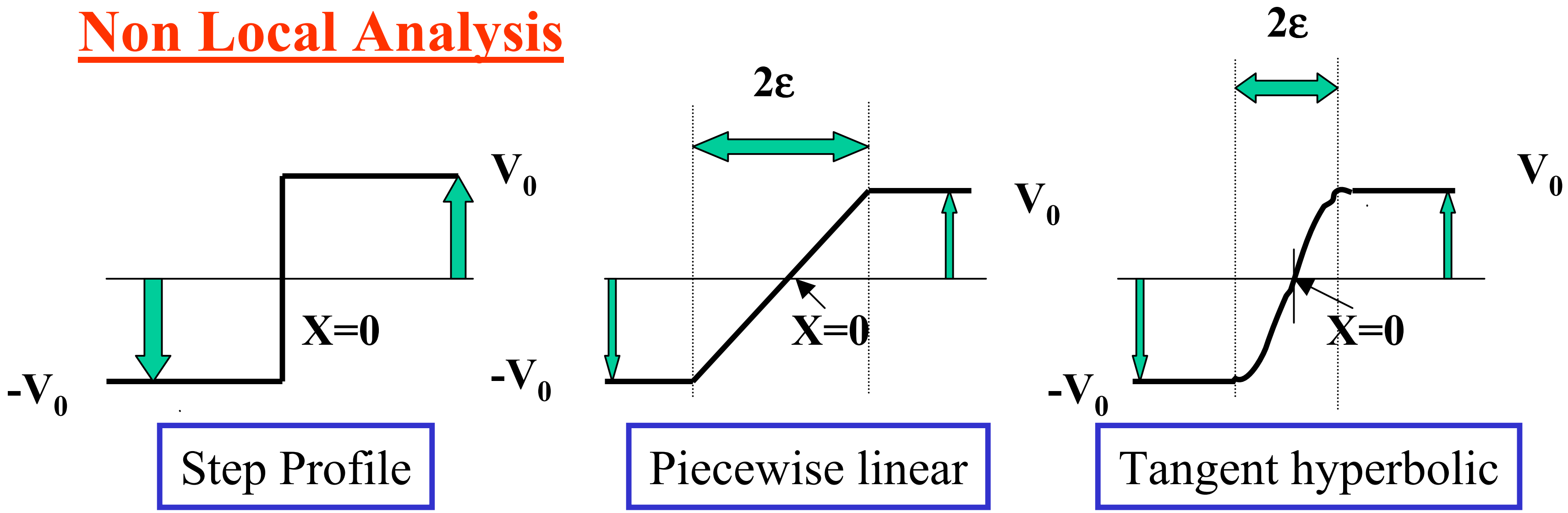

Summary of 2d linear Results (Contd.)

Step Profile:

$$\gamma^2 = \frac{k_z^{\ 2} V_0^{\ 2} (1 + 4\gamma_{0e} k_z^{\ 2})}{3 + 4\gamma_{0e} k_z^{\ 2}}$$

→ Growth rate increases monotonically with k_z. This gets restricted by finite shear width ε of equilibrium velocity profile

Limits:

$$\gamma_{0e} k_z^{\ 2} >> 1$$

→ Hydrodynamic K-H instability

$$\gamma_{0e} k_z^{\ 2} << 1$$

→ Magnetized character of electron fluid

Linear Sausage growth rates for finite shear width

Growth rate vanishes beyond some $k_z \varepsilon$ (Typically of order unity)

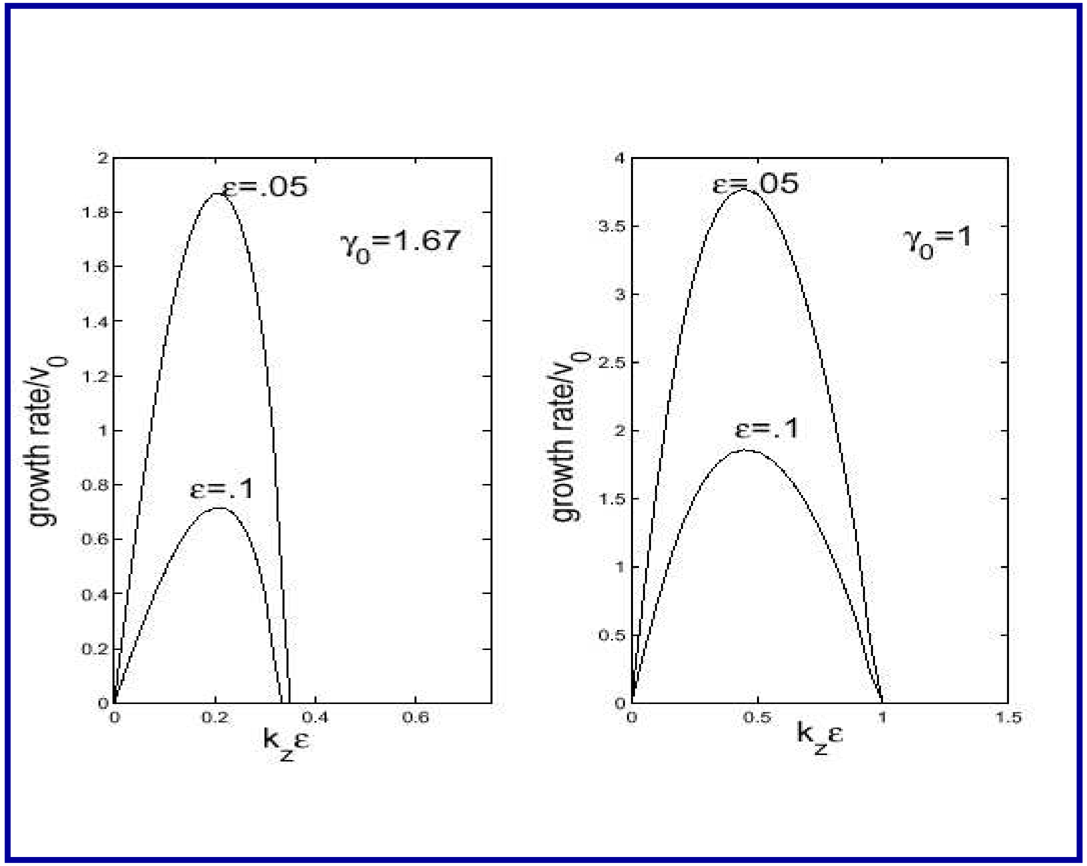

There is only one radial eigen-mode which is unstable.

Limit on $k_z\varepsilon$:

- For this mode ω is either purely imaginary or purely real. (Whistler waves not present as the variations along the field line are absent) Thus $\omega = 0$, defines the boundary where exchange of stability takes place.
- Substituting $\omega = 0$ and $v_0 = V_0 \tanh(x/\varepsilon)$ we have

$$\frac{d^2 B}{dx^2} - \left\{ k_z^2 - \frac{2}{\varepsilon^2} Sech^2\left(\frac{x}{\varepsilon}\right) \right\} B = 0$$

Which has an exact solution viz. $B \sim Sech(x/\varepsilon)$ only when $k_z^2\varepsilon^2=1$

Difference with MHD sausage instability

MHD: destabilization due to finite divergence of the plasma fluid flow. Responsible for the accumulation of density and the magnetic flux in the pinching region.

As can be seen from linearized MHD equations with the most important terms leading to sausage instability are

$$\frac{\partial B_{1y}}{\partial t} = -\frac{B_{0y}}{c} \nabla \cdot \mathbf{v}_1 ,$$

$$\rho \frac{\partial}{\partial t} \nabla \cdot \mathbf{v}_1 = -\frac{c}{4\pi} \{ B_{0y} \nabla^2 B_{1y} + B_{1y} \nabla^2 B_{0y} \} .$$

These equations lead to the dispersion relation

$$\omega^2 = \frac{B_{0y}^2 k^2}{4\pi\rho} - \frac{B_{0y}}{4\pi\rho} \frac{d^2}{dx^2} B_{0y} .$$

Difference (contd.)

In EMHD curl $\mathbf{v}_e$ is responsible for destabilization.

Taking the curl of electron equation of motion and using the Faraday's law, we have

$$\frac{\partial \mathbf{B}}{\partial t} = -\nabla \times \mathbf{E} = \frac{m_e}{e}\frac{d}{dt}\nabla \times \mathbf{v}_e + \nabla \times \frac{(\mathbf{v}_e \times \mathbf{B})}{c}.$$

Origin of nonlocal operators d^2B/dx^2 and d^2V_0/dx^2

3d Instability

$$\frac{d^2 v_{1x}}{dx^2} - (1+k^2)v_{1x} + \frac{k_y B_{1x}}{a} + \frac{k_y^2 B_0 v_{1x}}{\bar{\omega} a} + \frac{(v_0'' - v_0)k_z v_{1x}}{\bar{\omega}} = 0,$$

$$\frac{d^2 B_{1x}}{dx^2} - (1+k^2)B_{1x} - \frac{k_y v_{1x}}{a} = 0.$$

$$a = \bar{\omega} / (v_0' + B_0),$$

Permits whistler waves

For $k_y = 0$, Eqs. decouple. And $v_{1x} = ik_z B_y$ yielding 2d sausage Eq.

- Instability possible even in local regime. Driven by shear dV_0/dx when

$$D = -4k_y^2(v_0' + B_0)(v_0' - k_0^2 B_0) + (v_0'' - v_0)^2 k_z^2 < 0.$$

Linear kink results for generalized 3d perturbations

Maximum growth rate vs. k_z for various k_y.

C is the value of B_0 field at x = 0

Note k_y= 0, the solid line indicates the sausage result. It is zero at k_z = 0 and also has an upper limit on k_z beyond which it vanishes

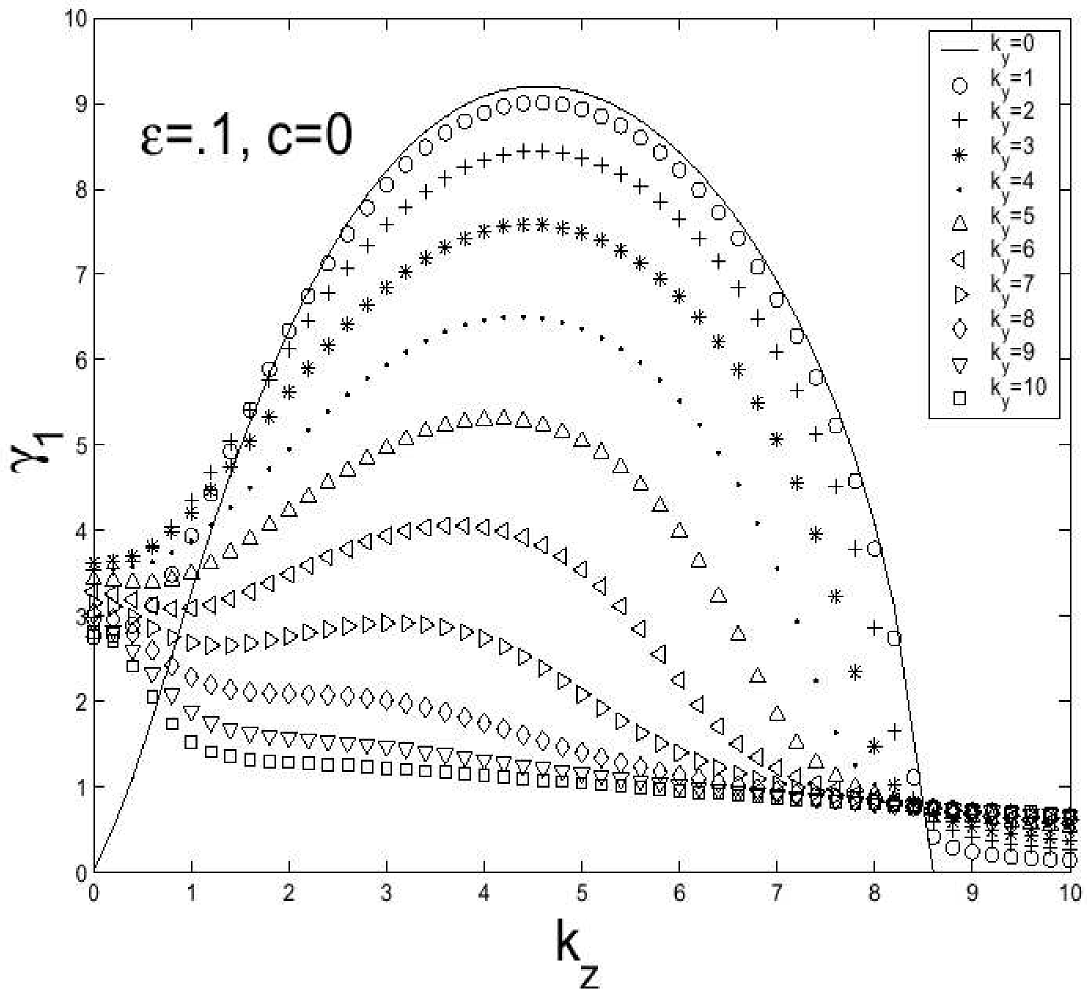

Second growing mode

The second maximum growth rate vs. k_z for various k_y (different line styles).

For k_y = 0, (the solid line style) the second growth rate vanishes. Thus there is only one growing mode for sausage like instability.

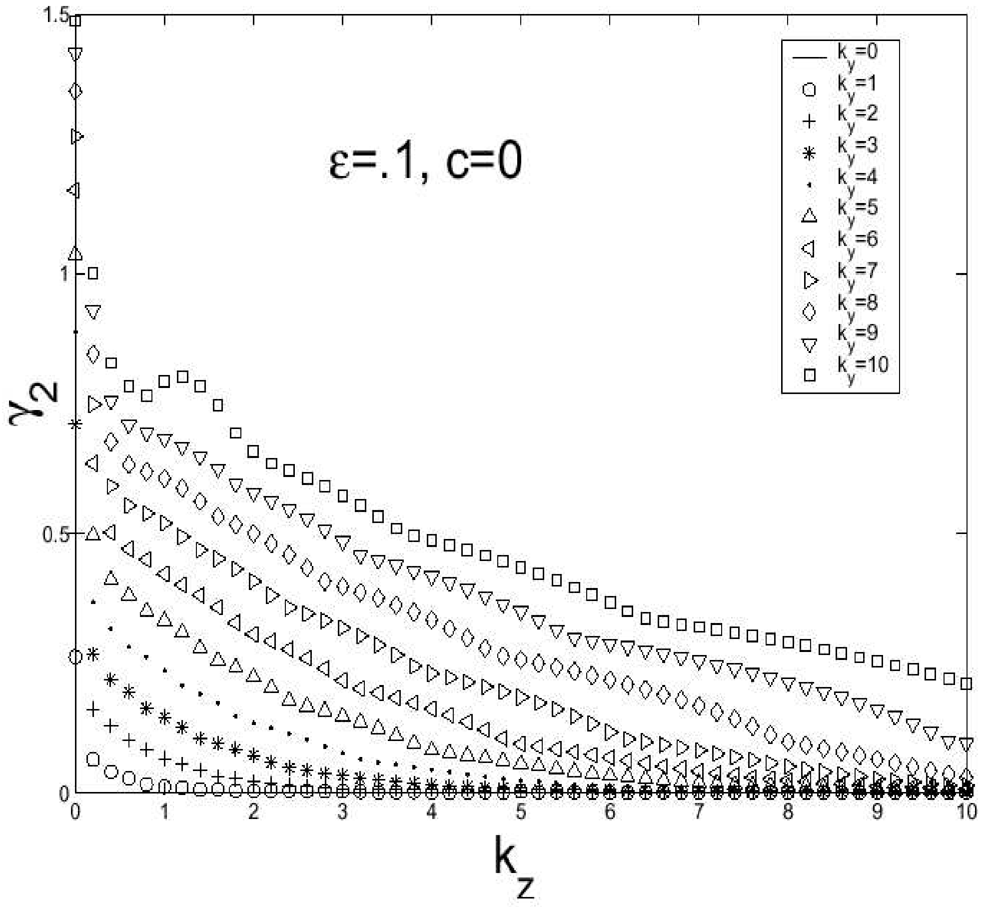

Radial eigen functions

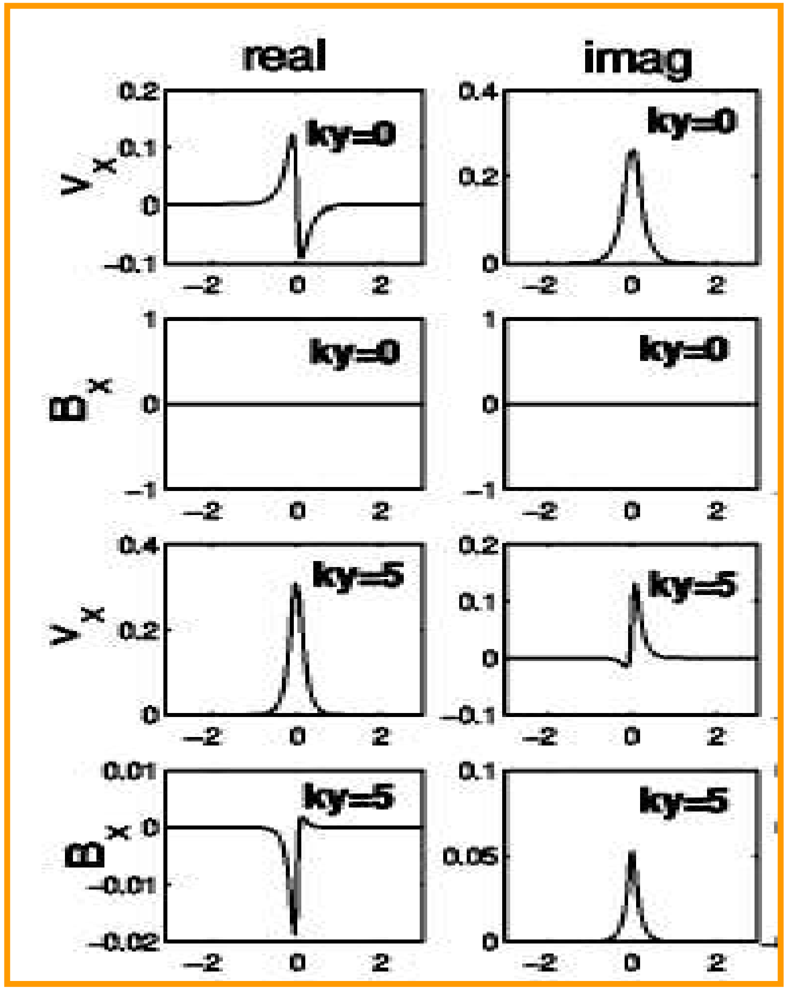

K_y =0 sausage mode hence only V_x is finite.

Nonlinear studies

2d simulations

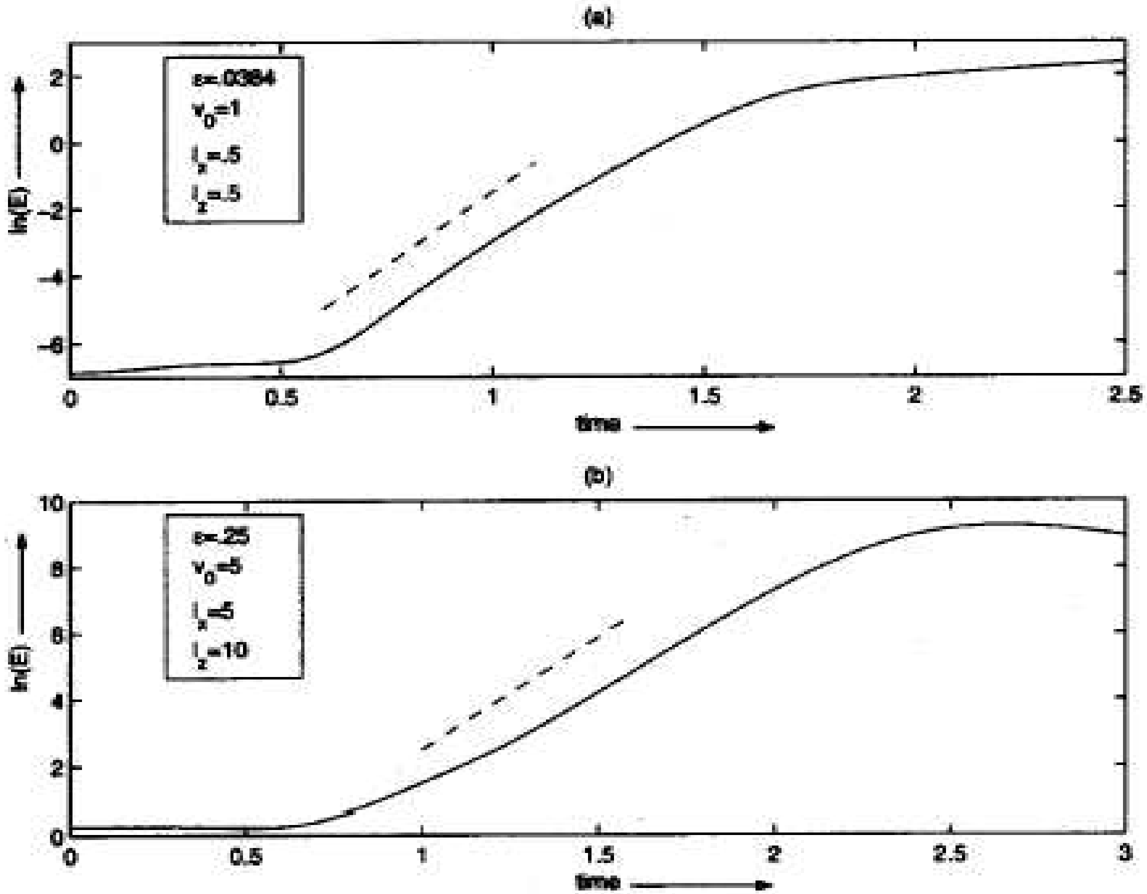

FIG. 6. The plot of $\log(E)=\log(\int\int \widetilde{B}^2 dxdz)/(\int\int dxdz)$ (E being the energy of perturbed magnetic field) with time for two sets of parameters. The dotted reference line has been drawn for comparison and indicates the analytical slope for the fastest growing mode obtained from Eq. (3).

Nonlinear Sausage Results

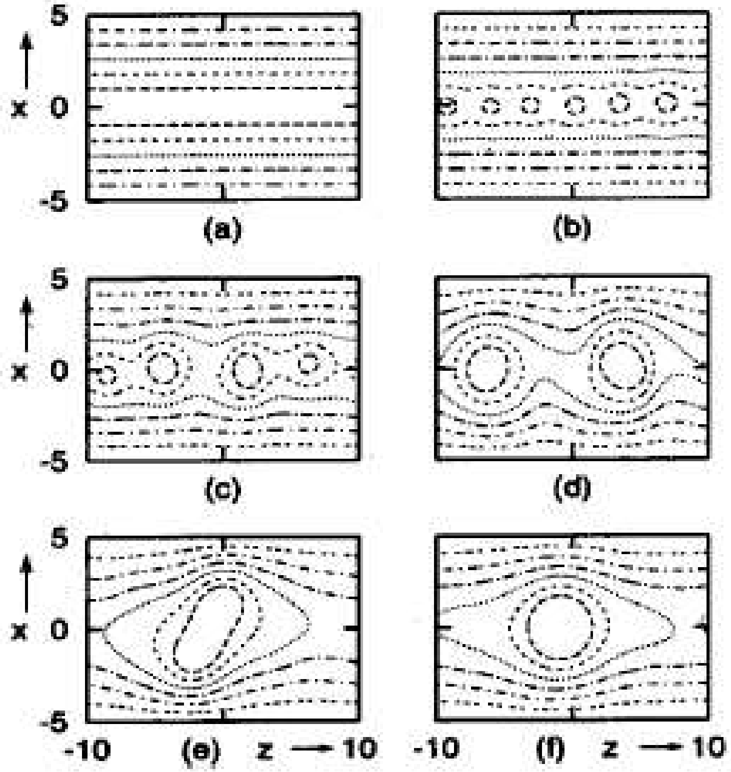

FIG. 7. The plot showing the coalescence of several magnetic islands with time at $t=0$, $t=5$, $t=7$, $t=10$, $t=25$, $t=40$ in subplots (a), (b), (c), (d), (e), and (f), respectively. For this case the parameters were $\epsilon=0.25$, $V_0=5$, $2L_x=10$, and $2L_z=20$.

Nonlinear velocity profile in 2d

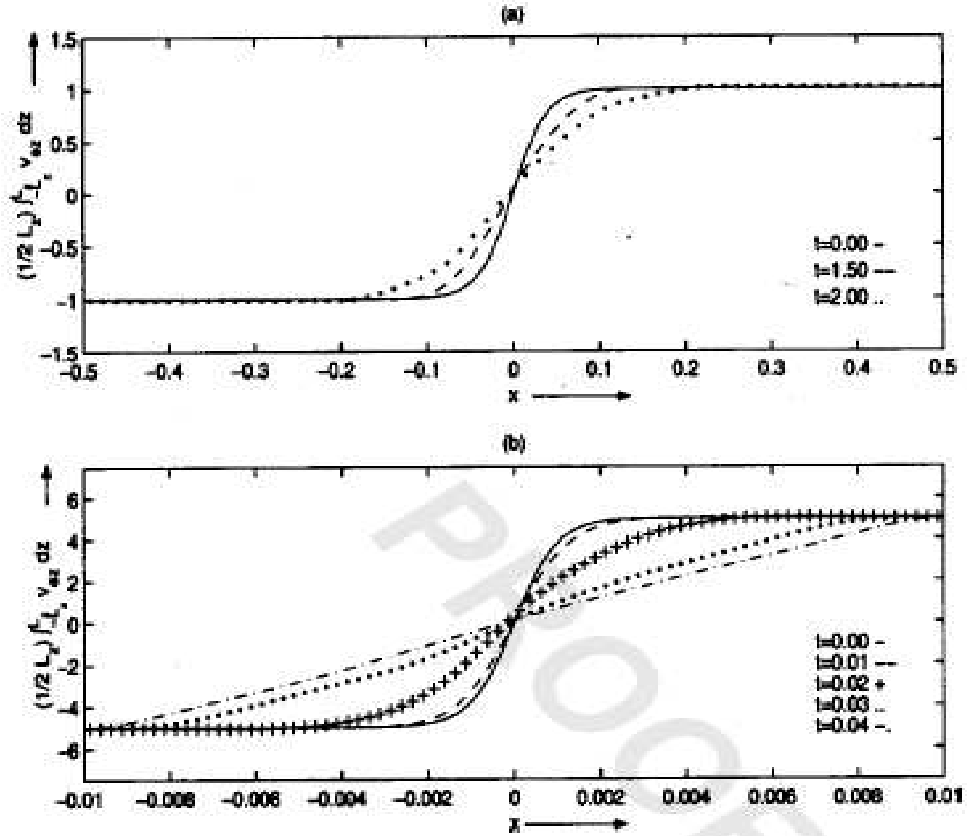

FIG. 8. The modifications of the equilibrium (z independent) velocity flow profile with time. Subplot (a) shows the evolution for the following simulation parameters $\epsilon = 0.0384$, $V_0 = 1$, $2L_x = 2L_z = 1.0$. Subplot (b) corresponds to $\epsilon = 0.001$, $V_0 = 5$, $2L_x = 0.02$, $2L_z = 1.0$.

Nonlinear Results (Contd.)

I. Cascade towards long scales
(linked with the existence of two non – dissipative square invariants of the evolution equation)

$$I_1 = \int (B^2 + (\nabla B)^2)\,dxdz$$

$$I_2 = \int ((\nabla B)^2 + (\nabla^2 B)^2)\,dxdz$$

II. Flattening of the shear profile

Increase in ε_{eff} saturates the instability.
flattening of shear → anomalous viscosity!!

3d simulations

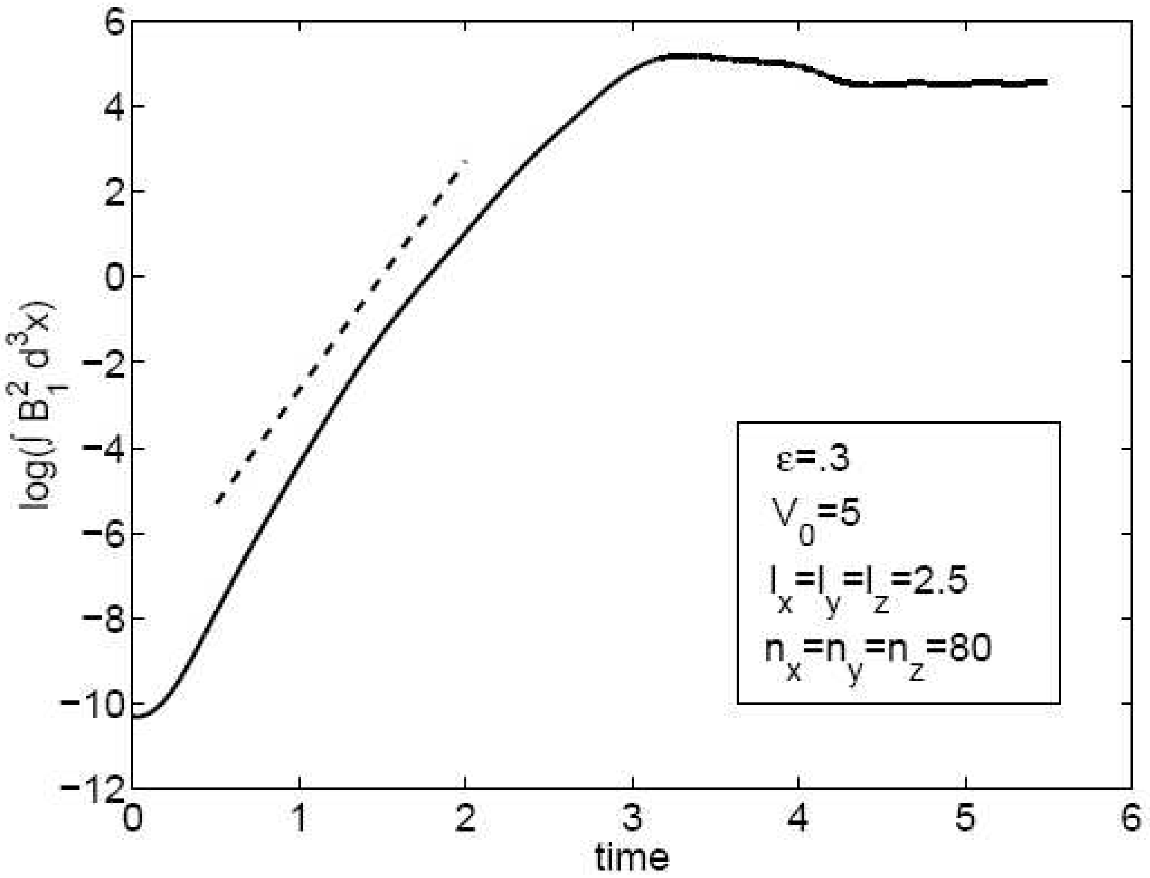

Axial velocity structure in 3d

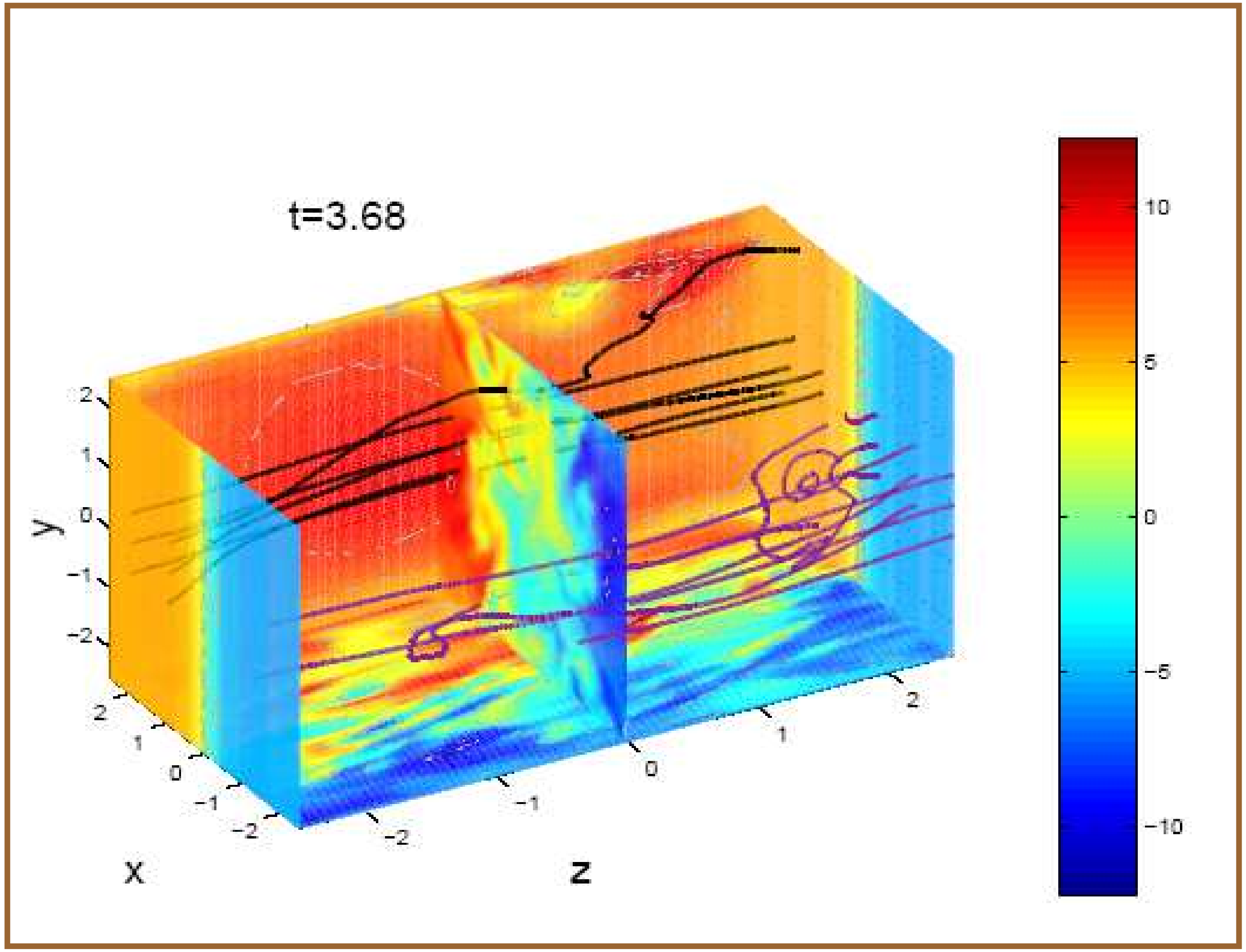

Evolution of axial velocity in x-y plane

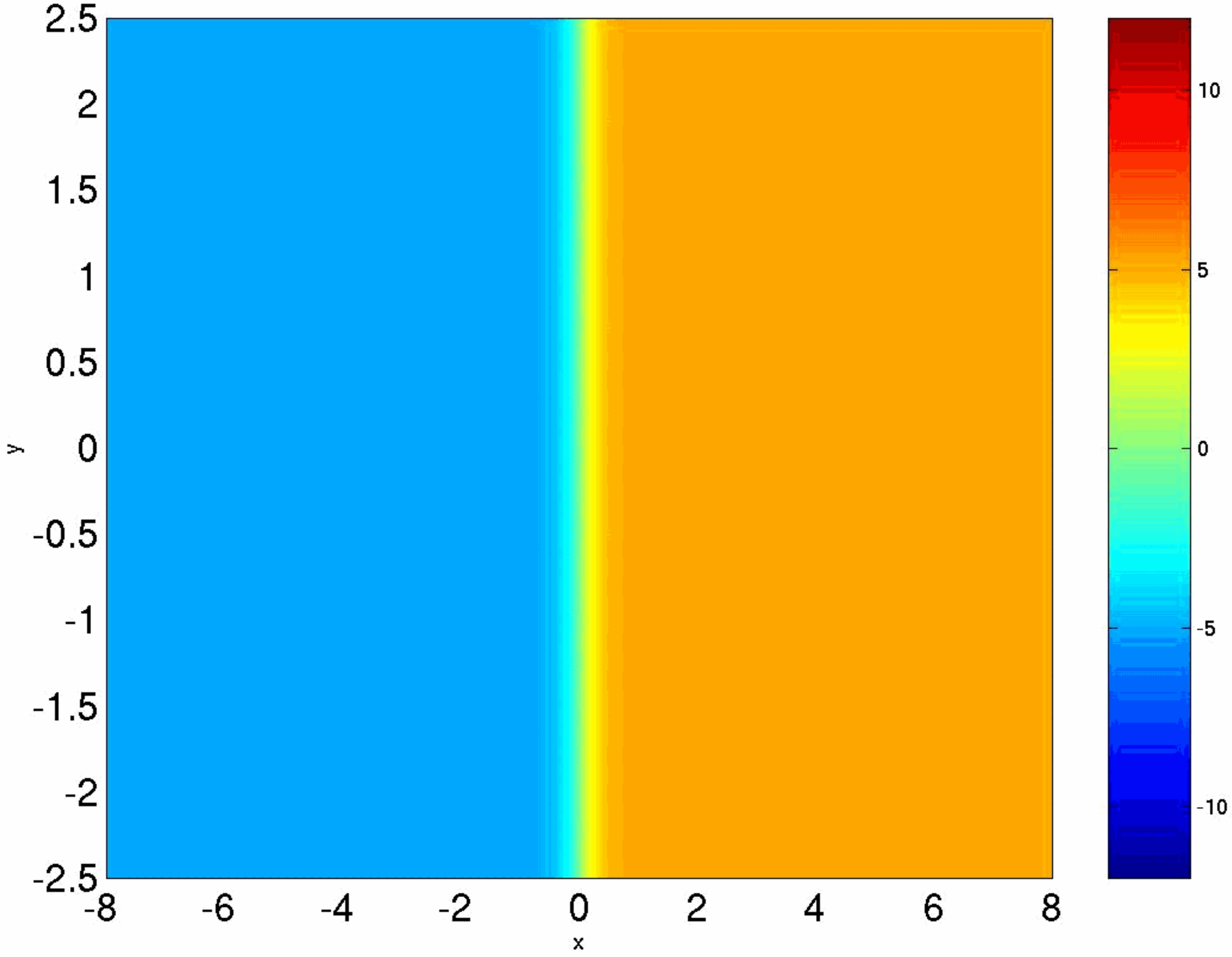

Evolution of axial velocity in x-z plane

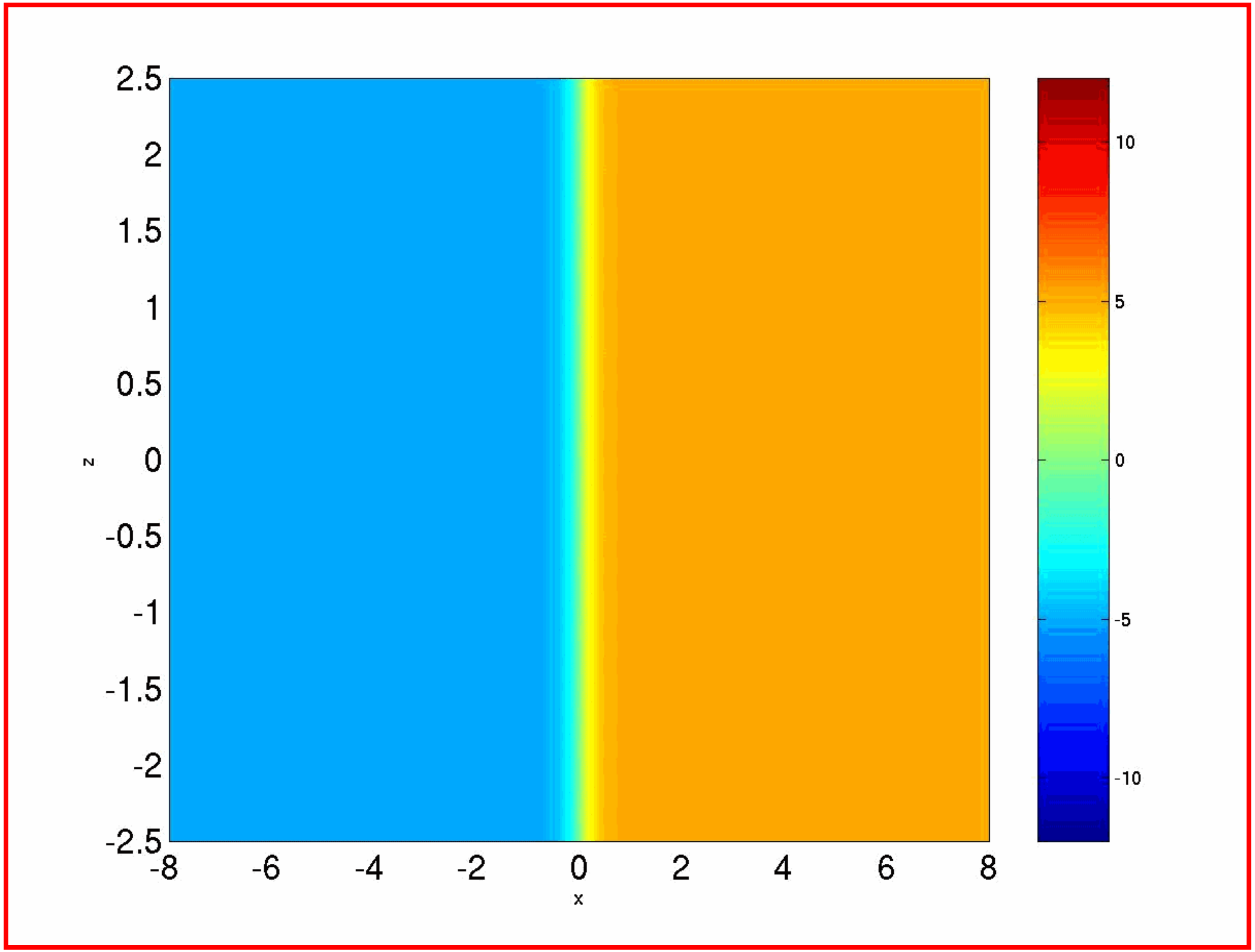

Evolution of velocity profile in 3d

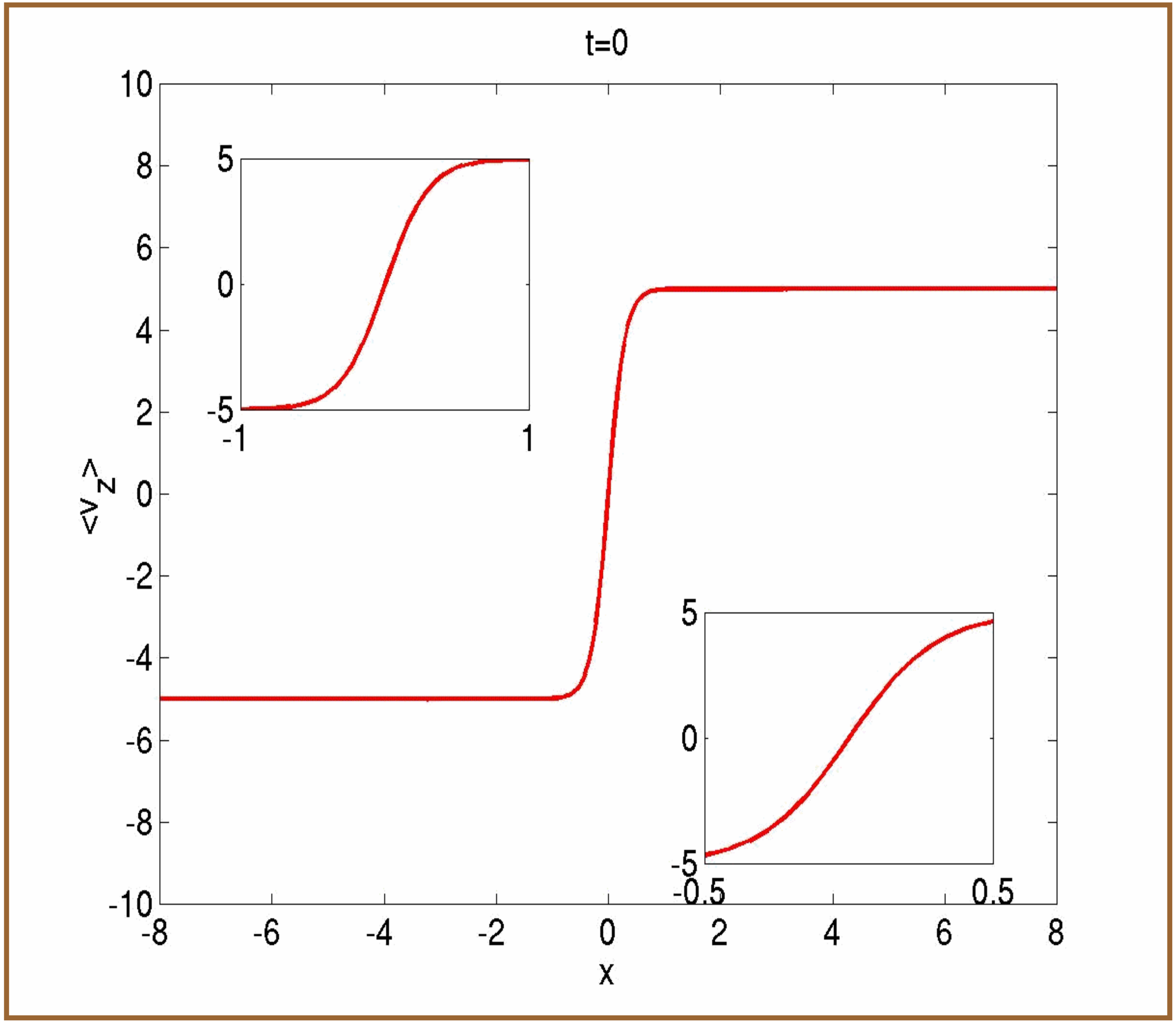

Reduction in current

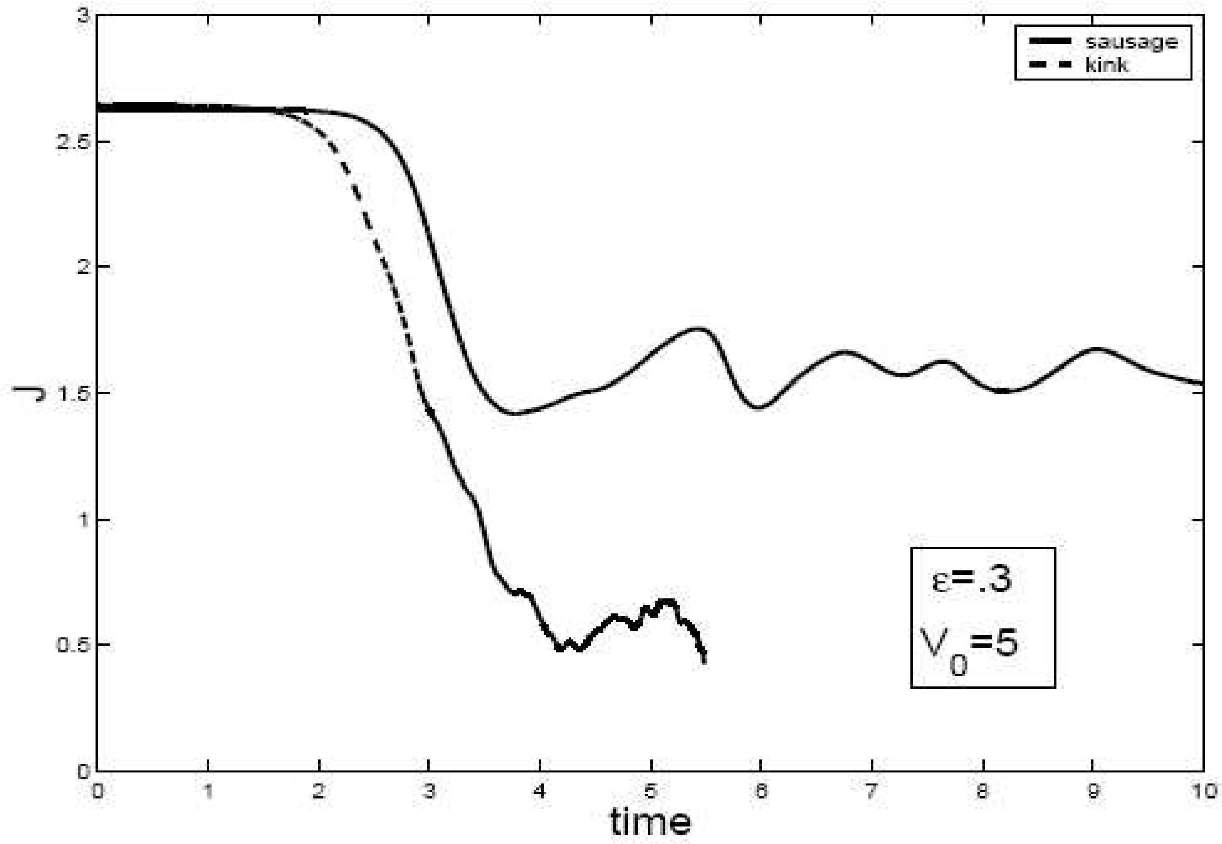

Estimate for the stopping distance

From simulation:

Velocity normalization by $c\omega_{ce}/\omega_{pe}$.

Parameters: Shear width $\varepsilon = 0.3$, $V_0=5$
Observation: 80% reduction in J; $\Delta J=2.0$ in $\Delta t = 5$.

For comparison with ignition expts:
$V_0=c$; hence $\omega_{ce}=\omega_{pe}/5$. ($\omega_{ce}$ el. Cyclo. fq. at B_{00})
For **n = 4** x **10^{21}**/cm^3**;** $\boldsymbol{\omega_{pe}}$ **= 3.6** x **10^{15}**/sec.
Time taken for 80% reduction = **5/ (3.6 x 10^{15}/5).**
Distance traversed in this time = L_{stop}= 2 micron

Typical estimates from simulation vary from 2 – 15 microns

Strong effect of Turbulence in reducing the stopping length .

Simplifications

We have ignored

- Curvature effects of the current filament ~ use slab x - y - z coordinate system.
- Relativistic nature of the fast electron beam.
- Plasma density gradient along the beam path.

These would be important for detailed quantitative investigations.

Summary

- The EMHD instabilities driven by velocity shear in 3d produce significant turbulence.
- The enhanced turbulence aids the process of stopping of the energetic electron flow implying a strong role of collective processes in the propagation of fast electrons through the plasma.

Instability and turbulence generation

Details in:

- A. Das and P. Kaw Phys. Plasmas **8** 4518 (2001).
- N. Jain, A. Das, P. Kaw and S. Sengupta Phys. Plasmas **10** 29 (2003).
- A. Das, N. Jain, P. Kaw and S. Sengupta Nuclear Fusion **44** 98 (2004).
- N. Jain, A. Das and P. Kaw Phys. Plasmas **11** 4390 (2004).
- 3d simulations still unpublished.

Iso - surface of B field

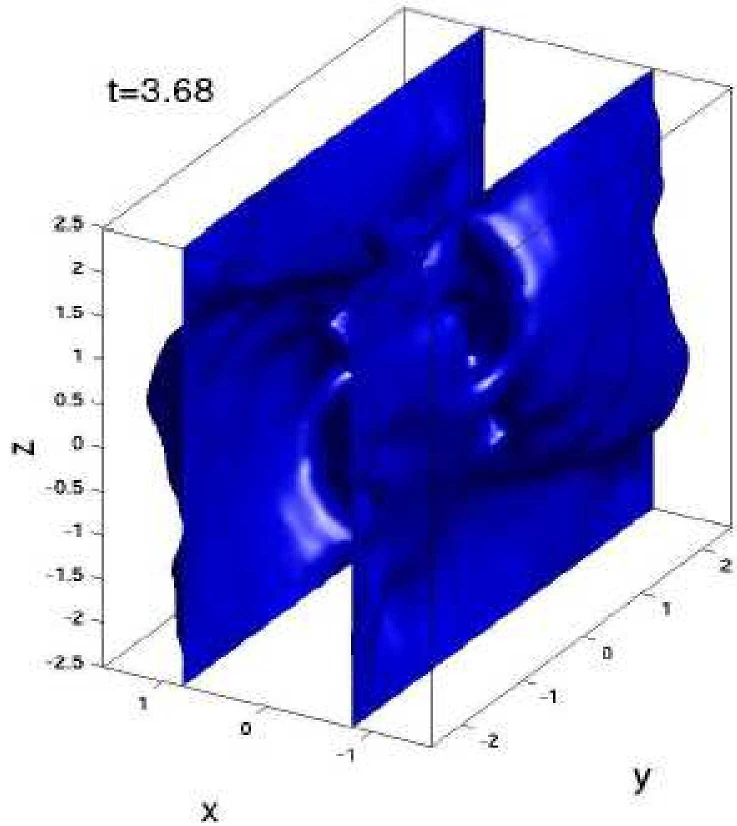

Profile Evolution in 3d

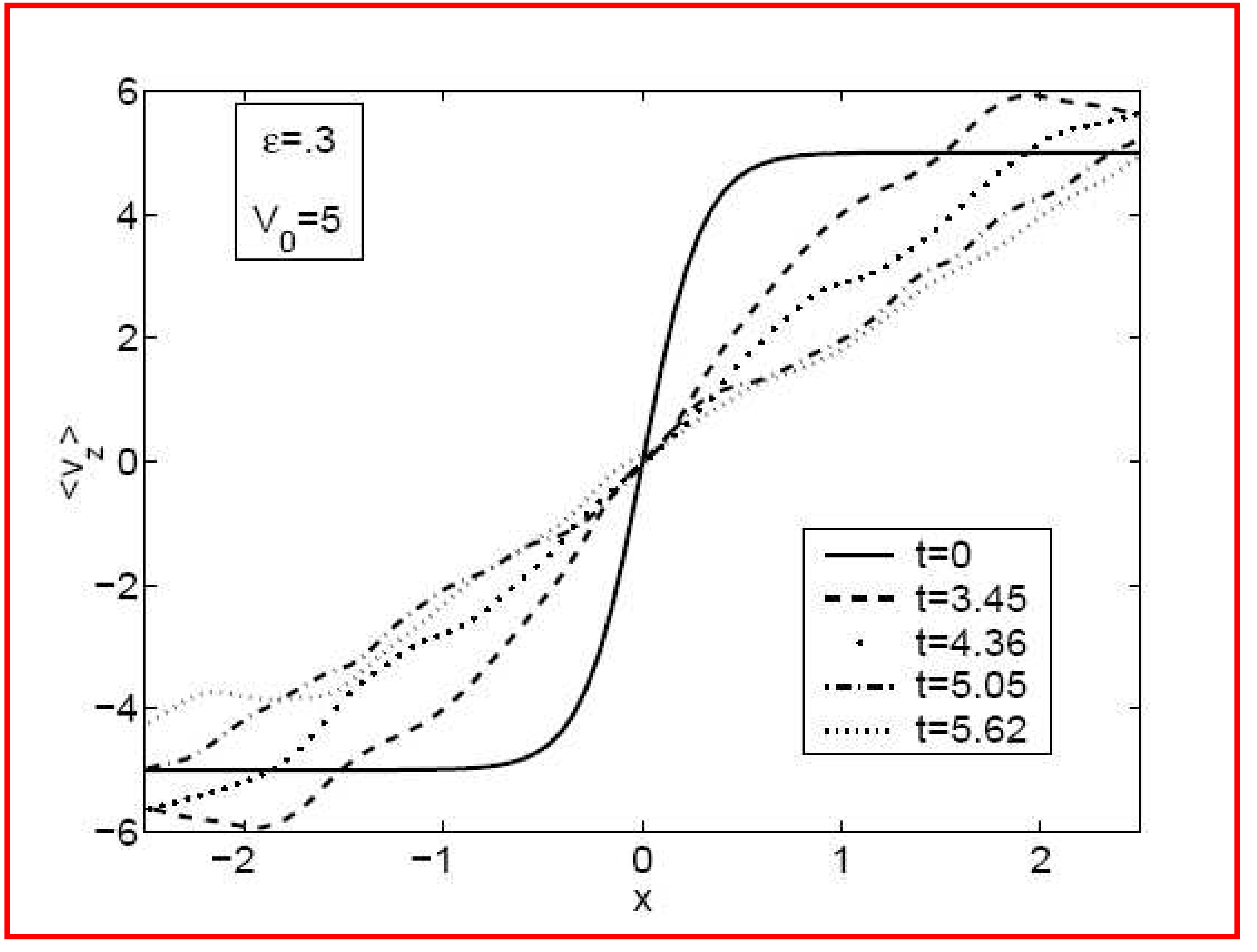

Nonlinear Results (Contd.)

Significant reduction in $\int_0^{L_x} V_0 \, dx$

But not complete stopping!!

Perhaps due to two dimensional constraints
~ coherence and lack of strong turbulence

3 dim simulations necessary to pin this down

Estimate for the stopping distance

From simulation:

Shear width $\varepsilon = 0.3$
Reduction J; $\Delta J=2.0$
Time duration $\Delta t = 5$

Assuming deceleration to continue at this rate ($a= \Delta J / \Delta t =2/5$)

Thus complete stopping would occur after traversing a distance of: $L_{stop} = J_{initial}^2/(2a) = 2.5^2/(4/5) = 7$

For $n = 4 \times 10^{21}/cm^3$; $\omega_{pe} = 3.6 \times 10^{15}/sec$

Skin depth $c/\omega_{pe} = 0.1\ \mu$

→ $L_{stop} = 7 \times 0.1\ \mu = 0.7\ \mu$

Quasilinear Estimate

The expression for ν_{eff} obtained from PIC can be obtained from simple quasilinear analysis of the EMHD equations

$$\frac{\partial V_0}{\partial t} + \nu_{eff} V_0 = \frac{e}{mc}\langle \delta B \times \delta V \rangle$$

$$\frac{\partial \delta V}{\partial t} + \nu_{eff} \delta V = \frac{e}{mc} V_0 \times \delta B$$

Assuming stationarity ~dropping the time derivatives and eliminating **δV** gives

$$\frac{\nu_{eff}}{\omega_c} \approx \frac{\delta B}{B_0}$$

Parameters (PIC simulations)

Parameters:

Laser power – 10^{12} Joules/sec;
Focused intensity – 10^{19} Watts/cm^2
Plasma density = 4.4 * $10^{21}/cm^2$
Laser wavelength = 1 micron.
Plasma fully ionized deuterium = 3680 m_e
Initial electron temperature = 10 KeV, ion temp = 0;
Transverse system size = 2.5 λ x 2.5λ
Longitudinal = 12 λ.
Linearly polarized wave, y polarization direction.
Periodic boundary condition in transverse direction.
Absorbing b.c. for fields and reflecting b.c. for particles in x direction.

Parameters (PIC simulations)

Spatial grid points 300x64x64. No. of Particles $2x10^{7}$.
20 particles /cell for ions and electrons.
Current in filament 5 kAmps. Relativistic factor =2.
$A = eA/mc^2 = 3.75$.
B_0 = 400 M Gauss (Peak Oscillating magnetic field).
Evolution upto $t = 12\tau$ as currents sheets – quasi –static B field energy = 0.1% B_0^2 . After $t = 16\ \tau$ current sheet breaks into filaments. Around $t = 20\ \tau$, strong quasistatic B field gets generated around 280 MG and blocks electrons from penetrating into plasma region.

Parameters (PIC simulations)

Alfven Speed $V_A = 10^9$cm/sec – in osc peak B field.
$= 10^9/7$ cm/sec - quasistatic

$\omega_{ce} = eB_0/m_e c =$

$$\frac{4.8\times 10^{10}\times 400\times 10^{6}}{9.1\times 10^{-28}\times 3\times 10^{10}} = 10^{16}\ / sec$$

$\omega_{ci} = 10^{16}/3680$ for He ions.

$C_s(10\ \text{KeV}) = 10^8$ cm/sec

$\omega_{ci} << \omega << \omega_{ce}$

Validity of the EMHD condition

$$\omega_{pe}^2 = \frac{4\pi n_0 e^2}{m} = \frac{4\pi\times 4.1\times 10^{21}\times (4.8)^2\times 10^{-21}}{9.1\times 10^{-28}} \approx \left(40\times 10^{14}\right)^2$$

Parameters (PIC simulations)

$$\frac{c}{\omega_p} = 0.5 \times 10^{-6}; \quad \frac{ck}{\omega_p} = 0.7; \quad V_0 = 0.4c$$

•This k corresponds to typical structure formed after a tearing instability and hence ε can be estimated from here as $2\pi(0.5/0.7)*10^{-6}$;
•Another estimate from $\varepsilon = 0.3\lambda = 0.3*10^{-6}$ (Pg.2 ms.).

Laser frequency $\omega = 2\pi/\tau = 10^{14} \sim 2*10^{15}$.
Typical growth time γ as observed $(28\text{-}16)\tau = 12\ \tau$.
$\gamma = 10^{14}/24\ \pi \sim k_z V_0$ (if it corresponds to the sausage growth time).

That leads to an estimate of k_z; $k_z\varepsilon$ turns out to be less than unity. Which means that the sausage condition is valid.

Parameters (fast ignition)

Typical target size before compression 1mm radii,
And density 10^{22}/cc solid density.
After compression 40 – 50 micron 10^{26}/cc

Calculations

Hot electron temperature T_{eV} = 3MeV,
Cold electron temperature T = 10KeV

$$\sigma = \frac{10^{-12}}{T_{eV}^{\ 2}} cm^2; \quad \sigma_{hot} = 10^{-25}$$

$$\nu_{ei} = n\sigma V = 10c = 3\times 10^{11}\ sec^{-1}$$

$$\lambda_{mfp} = \frac{1}{n\sigma} = \frac{1}{10^{26}\times 10^{-25}} = 1mm = 1000\ \mu$$

At 10 KeV

$$\nu_{ei} \approx \gamma_e^{3MeV}\left(\frac{10KeV}{3MeV}\right)^{-3/2} \sim 3\times 10^{11}(300)^{3/2} \sim 1.5\times 10^{15}$$

$$\frac{m_e}{m_i}\nu_{ei} \sim \frac{1.5}{3000}\times 10^{15} \sim 5\times 10^{11}$$

$$\tau_{ei}^{Energy} \sim 2\ p\ sec$$

Thus energy transfer to ions possible in psec duration

Propagation of fast electrons

Move at relativistic speeds!

- Will traverse distances larger than target size if only classical resistivity is operative.
- Additional anomalous slowing down essential for the success of the FI scheme!
- PIC simulations indicate the presence of anomalous slowing down mechanisms.

$$\frac{\nu_{eff}}{\omega_c} \approx \frac{\delta B}{B_0}$$

Estimate for the stopping distance

From simulation:

Shear width $\varepsilon = 0.3$
Reduction J; $\Delta J = 0.7$
Time duration $\Delta t = 10$

Assuming deceleration to continue at this rate
($a = 0.7/10 = 0.07$)

Thus complete stopping would occur after traversing a distance of: $L_{stop} = J_{initial}^2/(2a) = 4.5^2/0.14 = 145$

For **$n = 4 \times 10^{21}/cm^3$; $\omega_{pe} = 3.6 \times 10^{15}/sec$**
Skin depth c/ω_{pe} **= 0.1 μ**

→ **$L_{stop} = 145 \times 0.1\ \mu = 14.5\ \mu$**

Comparison with PIC results

Expression for effective collisional damping

$$\frac{\nu_{eff}}{\omega_c} \approx \frac{\delta B}{B_0} \approx 10^{-2}$$

for ◆$_c$ = 10^{15}

$$\nu_{eff} = 10^{13}$$

$$L_{stop} = \frac{c}{2\nu_{eff}} = 15\,\mu$$

Consistent with the 2d fluid simulation numbers

ICF Requirements (contd.)

If one chooses $n = n_s$, the solid density~ $5x10^{22}$, r =0.12cm.
E_i = 1.6 MJ, $\tau = r/V_s$~2 nsec.

Input power $P_i \sim E_i/\tau \sim 10^{15}$Watts.
Possible only with LASERS and Electron or Ion beams.

- Total electricity generation capacity India 10^{11}Watts; USA 10^{12} Watts.
- Total solar flux on earth ~ 10^{17}Watts

Things neglected in the estimation of P_i

- Coupling of driver (e.g. laser) energy to plasma.
- Electron ion coupling efficiency (laser heats only electrons).

Electron Magnetohydrodynamics(EMHD) Model: An Introduction

Applicability:

- Fast time scales phenomena ($\omega_{ci} << \omega << \omega_{pe}^2 / \omega_{ce}$) the upper limit ensures that displacement current can be ignored!
- Short length scales ($\rho_{ce} << k^{-1} << \rho_{ci}$)
- Unmagnetized stationary ions.

Problems in implementation

- Preheating of the central core by fast particles (compression difficult).
- Mixing of hot and cold fuels. (difficulty in producing ignition spark)

Reasons

- Nonlinear laser plasma coupling.
- Hydrodynamic stability of the implosion.

Single particle collisions

Experience friction due to collisions with background plasma particles.

Collisions amidst charged particles given by Rutherford cross section which decreases with increasing energy!!

The relativistic expression is

$$\frac{d\sigma^{ei}}{d\Omega} \approx \frac{Z^2}{4}\left(\frac{r_o}{\gamma\beta^2}\right)^2 \frac{1}{\sin^4(\theta/2)}$$

Where

$$\beta = \frac{v}{c}; \quad \gamma = \left(1-\beta^2\right)^{-1/2}; \quad r_o = \frac{e^2}{m_o c^2}$$

Classical estimates of stopping distance are a factor of 10 higher than typical size of the target.

Simple Estimate

Hot electron temperature T_{eV} = 1-3MeV,
Fusion Plasma density n = 10^{26}cm^3

$$\sigma = \frac{10^{-12}}{T_{eV}^{\ 2}} cm^2; \quad \sigma_{hot} = 10^{-25}$$

$$\nu_{ei} = n\sigma V = 10c = 3\times 10^{11} sec^{-1}$$

At T =3MeV

$$\lambda_{mfp} = \frac{1}{n\sigma} = \frac{1}{10^{26}\times 10^{-25}} = 1mm = 1000\ \mu$$

Thus stopping distance 100 – 1000 micron
for T_{hot}= 1 - 3 MeV beam.

Typical target size : 40 – 50 micron

Linear Analysis and Nonlinear Simulations

Presence of both 2 and 3d instabilities.

Sausage mode

- Excited by d^2V/dx^2
- Instability for modes with $k_z\varepsilon < 1$.
- For tanh profile maximal growth rate for these modes.
- Nonlinear cascade of power towards long scales.
- Turbulence weak (essentially absent).

Kink modes

- Even dV/dx finite is sufficient to excite the instability.
- A larger number and variety of modes.
- Direct cascade of power.
- Generation of strong turbulence.
- Better stopping.